Postprint of: Armaković S., Armaković S. J., Koziel S., Optoelectronic properties of curved carbon systems, Carbon, Vol. 111 (2017), pp. 371-379, DOI: 10.1016/j.carbon.2016.10.022

Optoelectronic Properties of Curved Carbon Systems

[1,*]Stevan Armaković, [2]Sanja J. Armaković and [3,4]Slawomir Koziel

[1] *University of Novi Sad, Faculty of Sciences, Department of Physics, Trg Dositeja Obradovića 4, 21000, Novi Sad, Serbia,*

[2] *University of Novi Sad, Faculty of Sciences, Department of Chemistry, Biochemistry and Environmental Protection, Trg Dositeja Obradovića 3, 21000, Novi Sad, Serbia,*

[3] *School of Science and Engineering, Reykjavik University, 101 Reykjavik, Iceland*

[4] *Faculty of Electronics, Telecommunications and Informatics, Gdansk University of Technology, 80-233 Gdansk, Poland*

Abstract: Systematic investigation of optoelectronic properties of curved carbon systems has been performed and the results have been compared with the representatives of flat carbon systems. Moreover, the application of third order dispersion corrected density functional tight binding method (with third order corrections of self-consistent charges) including Becke-Johnson dumping (DFTB3-D3(BJ)) has been validated in order to obtain reliable dimer structures for the calculations of charge transfer rates. Optoelectronic properties encompassed calculations of reorganization energies, energy difference between the singlet and triplet state, first hyperpolarizabilities, whereas the charge transfer rates have been calculated according to the equation of Marcus semi-empiric approach. The obtained results indicate that a wide list of outstanding features of buckybowls could be expanded for optoelectronic properties as well. Furthermore, it has also been shown that correlation in the form of the second order exponential decay between electron transfer rates and the specific structural property of buckybowls exists. This allows for computationally inexpensive assessment of electron hopping rates.

* Corresponding author. Tel: +381 631019036. E-mail: stevan.armakovic@df.uns.ac.rs (Stevan Armaković)

1. Introduction

Modern science cannot be imagined without carbon-based structures. By all means, carbon is the central figure in organic chemistry and it has a potential to be applied in virtually all important scientific areas: material science, electronics, optoelectronics, medicine and biology [1]. Researchers have been focused on the carbon based materials ever since the 1950s, while milestones like a discovery of fullerenes, nanotubes and graphenes have been constantly shaking the entire scientific community in a positive way. Curvature of fullerenes and nanotubes practically opened a new chapter in the area of exotic organic molecules whose main characteristic is a bowl shaped structure [2-4]. These molecules are also known as buckybowls.

The first curved organic molecule, corannulene, was discovered in 1966 by Barth and Lawton [5, 6], but the interest in its physio-chemical properties ended soon. However, discovery of fullerenes and nanotubes triggered the interest in curved structures and the number of papers related to these structures dramatically increased. In 2001 Priyakumar and Sastry reported a theoretical study on possibilities to synthesize the structure of $C_{21}H_{12}$ buckybowl called sumanene, whose previous synthesis attempts by several research groups were not successful [7]. This typical representative of buckybowls was successfully synthetized two years later by the Sakurai's group [2] and in this regard it is important to mention that experimental conditions for its synthesis were characterized as mild. After the successful synthesis, scientific community became richer in many sumanene-based buckybowls [8-11].

Buckybowls possess an entire set of interesting properties and some of them include specific charge distribution, bowl-to-bowl inversion (b2b-i) and benzylic carbons [12]. Due to bowl-shaped structure, the more negative charge is located on its concave side. As a result, these structures feature two surfaces with considerably different adsorption properties [13, 14]. B2b-i of buckybowls means that they practically oscillate between two bowl-shaped ground states via a flat transition state. What is even more important is that this phenomenon occurs with certain frequency and that b2b-i ~~inversion~~ energy is directly related to the bowl-depth [15-18]. Some buckybowls, such as sumanene, possess benzylic carbon atoms due to which various functionalization procedures are readily available [19]. These, in turn, permit fine adjustment of the b2b-i energy.

Buckybowls are also interesting for the field of organic electronics. For sumanene and its trimethylated derivative, high electron conductivity has been reported [20, 21]. Also, very high

anisotropy was detected with much better electron conductivity along the π-bowl stacking axis [20]. In its crystal form, sumanene molecules are π-stacked along the bowl depth direction. Sumanene's conductivity along the π-stacking axis is 9.2 times larger than the conductivity in the direction perpendicular to the π-bowl stacking axis. The first liquid crystallization of corannulene has been reported by Miyajima et al. in 2009 [22], while buckybowls where one or more carbon atoms are replaced by the main group element exhibit unique optoelectronic properties [23].

Although buckybowls possess very interesting properties there is a lack of systematical theoretical studies concerning their specificities. The two important systematic studies, which stimulated the present work, were conducted by Purushotham and Sastry [1], and Jose et al. [24]. The first study addressed estimation of optoelectronic properties of sumanene and corannulene buckybowls, fused by acenes, and based on the calculations of reorganization energies. It emphasizes a potential of sumanene and corannulene as organic light emitting diode OLED materials. Nevertheless, the study lacks any calculations of the charge transfer rates between the investigated structures. On the other hand, Jose et al. investigated stacking interactions between 16 buckybowls and fullerenes. In their study, they have validated the employment of a dispersion corrected self-consistent charge density functional tight-binding (SCC-DFTB-D) method for investigating interaction energies between buckybowls and fullerenes. Motivated by the results of these two studies, in this work, we carried out detailed investigation of the optoelectronic properties of all 16 buckybowls studied in [24], including the charge transfer rates. In order to compute the charge transfer rates we also needed dimer structures of buckybowls. Dimer structures have been obtained by DFTB3-D3(BJ) method and DFT-D3 methods. D3 stands for the third-order empirical dispersion corrections, whereas BJ stands for the Becke-Johnson dumping. The obtained results have been compared, which allowed us to validate the much faster DFTB3 method for obtaining dimer structures of buckybowls. DFTB3 method stands for the SCC-DFTB method where self-consistent charges are used with the third order corrections, which is an improvement over the DFTB method utilized in the study of Josa et al.

2. Computational details

All DFT calculations have been executed using the Jaguar 9.0 program [25], as implemented in Schrödinger Materials Science Suite 205-4 (SMSS), and Amsterdam Density Functional Molecular Modeling Suite (ADF) 2016 [26-28]. The monomer units of buckybowls have been

first geometrically optimized with Jaguar using the B3LYP [29] exchange correlation functional with the 6-31G(d) basis set, with fine grid density, and increased integral accuracy. Vibrational analysis has been also conducted in order to ensure that the true ground states have been identified. The monomer units of buckybowls have also been optimized at the DFTB3 level of theory. These results allowed us to obtain information on dipole moments and bowl depths so that the two levels of theory could be compared.

Subsequently, using the corresponding optoelectronics module of Schrodinger Materials Science Suite, the relevant optoelectronic quantities have been calculated such as electron and hole reorganization energies and the energy separation between the lowest excited singlet (S1) and the triplet (T1) states, ΔE(S1–T1) gaps. Calculation of the optoelectronic properties have been performed within the defined screening model, as implemented in SMSS. The detailed data on the model can be found in [30].

In order to calculate the charge hopping rates between buckybowl structures, beside reorganization energies, we also needed information about the charge transfer integrals; that, in turn requires the dimer structures of the buckybowls. Starting geometries of all 16 investigated buckybowls have been obtained by placing one buckybowl above another along the direction of the bowl depth. Since dimer structures are large, firstly we optimized them at the DFTB3-D3(BJ) [31-34] level of theory using the ob3.1 parameter set [35], as implemented in ADF 2016. After that, we also performed geometrical optimizations of the dimer structures at the DFT level of theory with dispersion-corrected PBE-D3 functional and the DZP basis set [36, 37]. In these cases, frequency calculations within analytic approach [38-40] have been also performed in order to assure that the true ground states were located. In all cases but one, for a dimer structure denoted with number 9, only positive frequencies have been obtained. Dimer structure 9 was then re-optimized with somewhat smaller basis set, DZ, and vibrational analysis yielded only positive frequencies.

After obtaining the dimer structures, charge transfer integrals have been calculated in dimmer frontier approximation for dimer structures obtained at both DFTB3-D3(BJ) and DFT-D3 levels of theory, which finally allowed calculation of the charge hopping rates. In order to compare the results and to assess the potential of buckybowls, the same procedures were conducted for typical representatives of flat carbon systems with perspective physio-chemical properties – pentacene and coronene.

3. Results and discussion

3.1. Geometrical parameters and validation of DFTB3 level of theory for buckybowls

In order to calculate charge transfer rates from one buckybowl to another it is necessary to obtain their dimer structures, which can be a very demanding task in terms of the necessary computational resources. Fortunately, the DFTB3-based method is significantly faster than the DFT approach and beside the calculations of optoelectronic quantities the purpose of this study was to validate the DFTB3-D3(BJ) approach for obtaining reliable monomer and dimer structures for further calculations. All investigated buckybowls optimized with the B3LYP functional and 6-31G(d) basis set are presented in Figure 1.

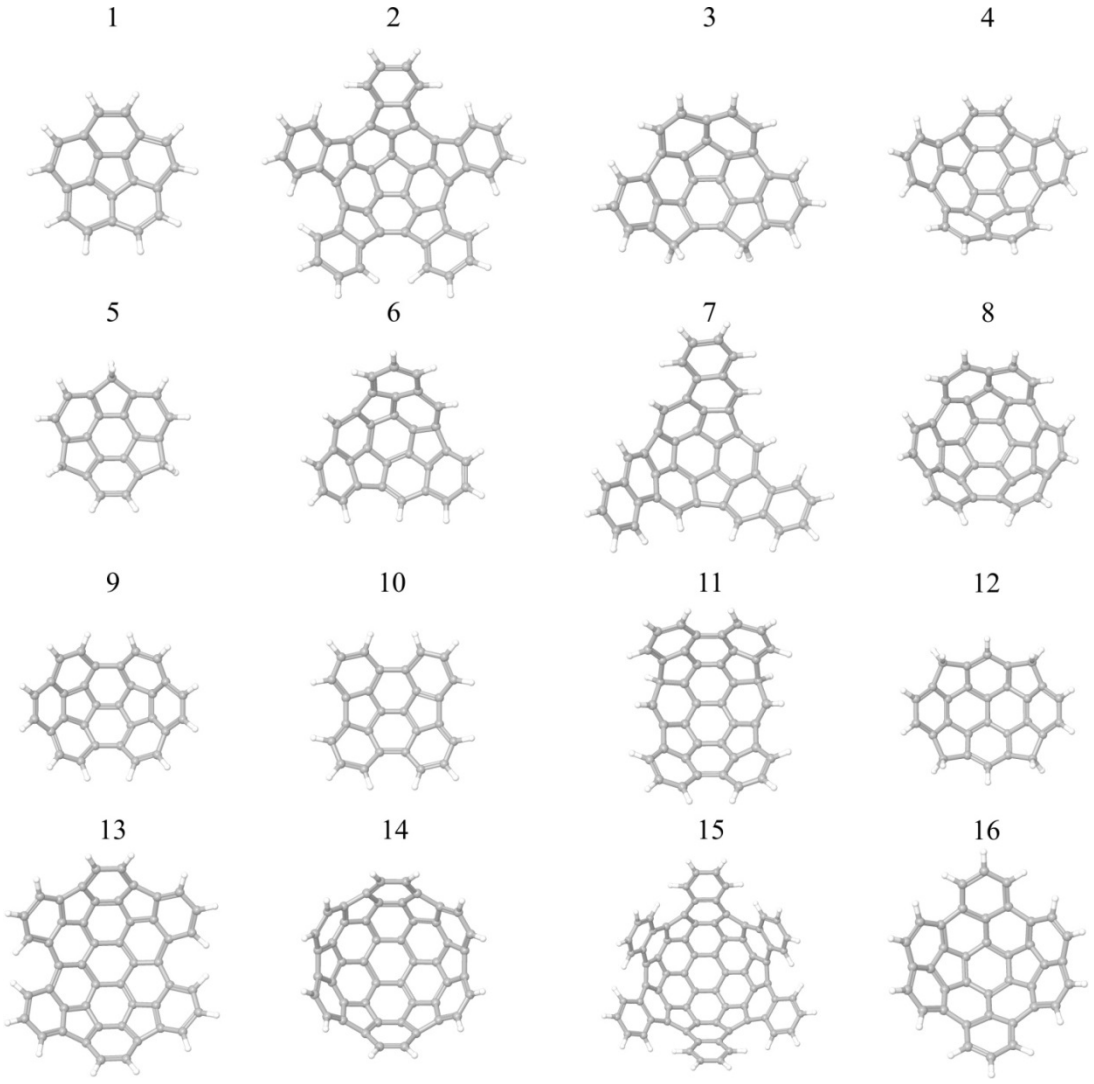

Figure 1. Structures of investigated buckybowls obtained at the DFT level.

The best way to investigate to what extent a given level of theory is efficient to obtain reliable geometries is to compare the results. Certainly, the most typical feature of buckybowls is the bowl depth. In the literature data, including some of our own works, it has been demonstrated that a very important process, b2b-i, principally depends on this structural feature [16-18, 41-44]. Namely, higher bowl depth leads to the higher energy barrier for the bowl inversion. These results are very important because frequency of b2b-i oscillations depends on the b2b-i barriers, while, at the same time, the aforementioned oscillations could be of great importance for the practical application of buckybowls in the area organic electronics. What is even more important is that the bowl depth, and therefore b2b-i barriers, can be finely tuned by structural modifications of the buckybowls. For example, it has been demonstrated that modifications of the sumanene buckybowl at its benzylic positions can lead to the increase or decrease of the bowl depth [18, 44]. Therefore, it was important to compare the bowl depths as obtained with DFTB3 approach, Table 1.

Table 1. Bowl depths of buckybowls and distances between buckybowls in dimer structures

Structure	Monomer Bowl Depth @ DFTB3/3ob.3.1 [Å]	Monomer Bowl depth @ DFT/B3LYP [Å]	Dimer distances @ DFTB3-D3(BJ)/3ob.3.1 [Å]	Dimer distances @DFT/PBE-D3 [Å]
1	0.92	0.84	3.55	3.46
2	3.74	3.55	4.16	4.05
3	2.68	2.27	3.92	3.88
4	2.95	2.53	4.33	4.10
5	1.20	1.12	3.71	3.65
6	2.62	2.40	4.05	3.93
7	3.82	3.81	4.02	3.94
8	2.95	2.92	4.89	4.70
9	2.77	2.71	4.12	3.92
10	1.53	1.25	3.56	3.49
11	3.57	3.43	4.43	4.24
12	2.18	2.15	3.94	3.77
13	2.23	2.09	3.78	3.58
14	3.26	3.23	5.07	5.01
15	4.90	4.80	4.53	4.51
16	2.51	2.44	4.10	4.00

The results in Table 1 indicate excellent performance of the DFTB3 approach for the buckybowls concerning the bowl depths. The two methods yielded very similar results and this very good agreement is also visualized in Figure 2, where the values obtained by both methods were correlated. In this case, a very high correlation coefficient of 0.997 has been obtained confirming the validity of the DFTB3 method for geometrical optimization of buckybowls. It was especially interesting to note that DFTB3 performed so well in the cases of the largest buckybowls. For example, discrepancy between two methods in the case of the largest buckybowl, denoted with number 15, was only 0.1 Å.

Concerning the dimers of buckybowls, the most important structural feature is certainly the distance between buckybowls. Taking into account the model according to which the charge transfer rates will be calculated later, this is actually the most important structural parameter and for the overall validation of the DFTB3-D3(BJ) approach it was very important to obtain good agreement with the DFT-D3 level of theory, cf. Figure 3.

In order to obtain dimer structures with the DFT approach we have used the D3 [45, 46] corrected version of the PBE functional [34]. This level of theory yields very similar results as B3LYP-D3, as shown in our study of adsorption properties of sumanene molecule [47], but in the same time it is much faster than B3LYP-D3.

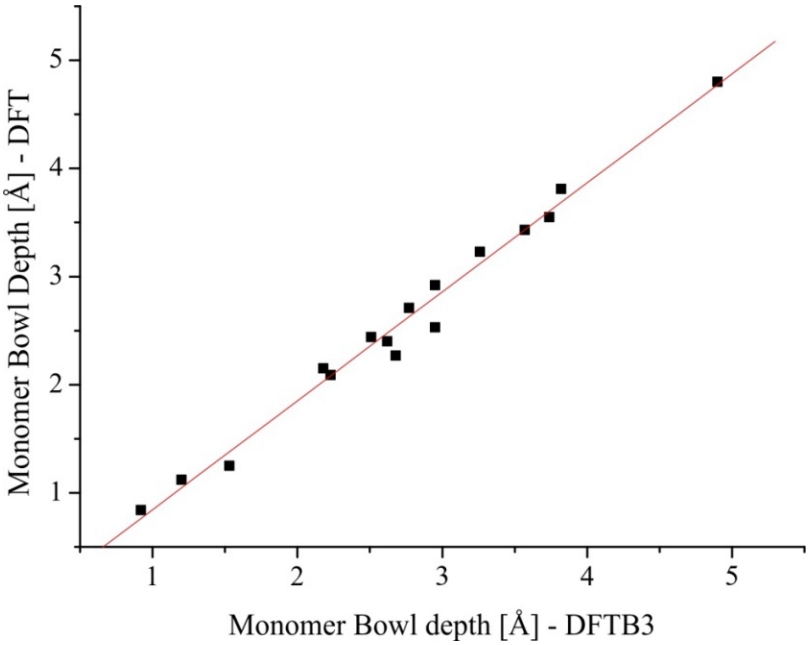

Figure 2. Comparison of DFTB3 and DFT/B3LYP bowl depths.

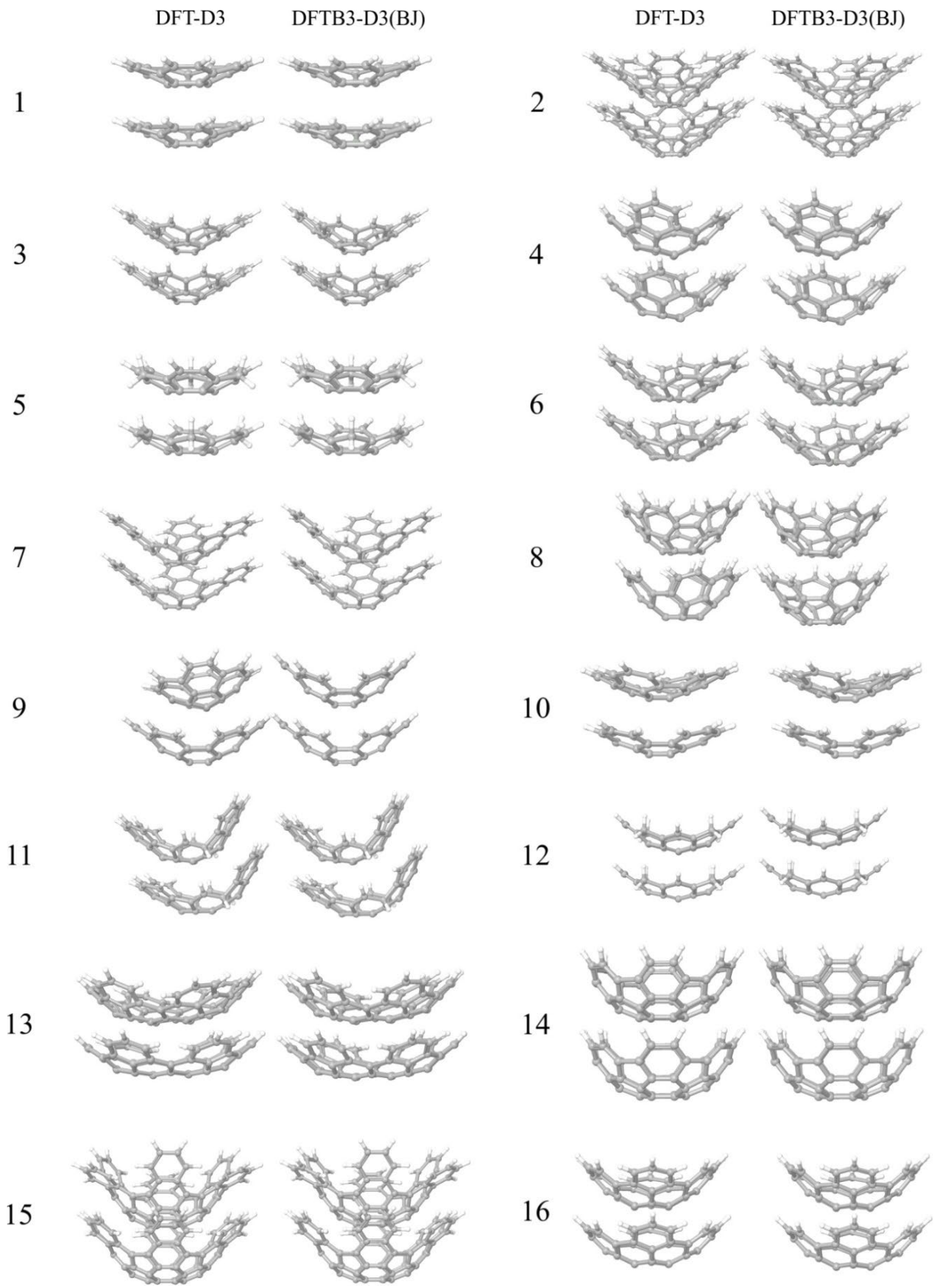

Figure 3. Dimer structures obtained with DFTB3-D3(BJ) and DFT/PBE-D3 levels of theory

Compared distances between buckybowls in dimer structures are provided also in Table 1, whereas the dimer structures obtained with DFTB3-D3(BJ) and DFT/PBE-D3 levels of theory are visualized in Figure 4. Concerning the dimer structures, it can be also concluded that DFTB3-D3(BJ) produced reliable results and again very high correlation coefficient between the two methods has been obtained.

3.2. Optoelectronic properties of monomer structures

Efficient electronic devices and materials are characterized by high charge mobility and are suitable for charge injection [48]. Charge mobility at room temperatures can be efficiently assessed employing DFT calculations [49]. In this regard, the most important mechanism is a so-called hopping mechanism and within this mechanism charge hopping rates, k_{CT} (k_{CT}^{+} for holes and k_{CT}^{-} for electrons), can be calculated employing the Marcus semi-empiric approach as follows [50, 51]:

$$k_{CT} = \frac{4\pi^2}{h}\frac{1}{\sqrt{4\pi\lambda k_B T}}t^2 \exp\left[\frac{-\lambda}{4k_B T}\right] \qquad (1)$$

where λ denotes reorganization energies of holes (λ^{+}) or electrons (λ^{-}), whereas t is the charge transfer integral (or charge coupling). These two quantities principally determine the charge transfer rates and brief analysis of equation (1) indicates that in order to obtain the highest possible transfer rates λ needs to be minimized, while t should be maximized.

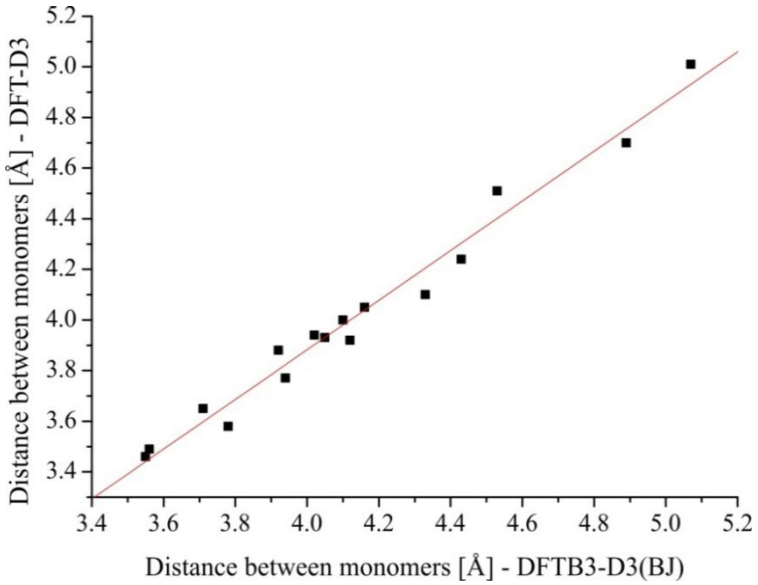

Figure 4. Compared distances between buckybowls in dimer structures

In this work, reorganization energies have been calculated according to the following equations (2-4):

$$\lambda_1 = E^0\left(G^*\right) - E^0\left(G^0\right) \quad (2)$$

$$\lambda_2 = E^*\left(G^0\right) - E^*\left(G^*\right) \quad (3)$$

$$\lambda_i = \lambda_1 + \lambda_2 \quad (4)$$

where $E^0\left(G^0\right)$ and $E^*\left(G^*\right)$ are the ground state energies of the neutral and ionic states, respectively. $E^0\left(G^*\right)$ is the energy of the neutral molecule at the optimal ionic geometry, while $E^*\left(G^0\right)$ is the energy of the charged state at the optimal geometry of the neutral molecule. Reorganization energies and ΔE(S1–T1) gap values are provided in Table 2, together with the values of dipole moments and the first hyperpolarizabilities.

Table 2. Reorganization energies, dipole moments, the first hyperpolarizabilities and ΔE(S1–T1) values of buckybowls

Structure	λ^+ [eV]	λ^- [eV]	Dipole moment [D]	Hyperpolarizability [a.u.]	ΔE(S1–T1) [eV]
C1	0.3860	0.2508	1.6637	75.5657	0.7575
C2	0.0998	0.1777	3.3432	237.9439	0.4620
C3	0.1527	0.2414	3.2079	77.9124	0.9041
C4	0.2102	0.2661	3.8671	189.8181	0.5402
C5	0.1956	0.3620	1.9462	102.4921	1.1998
C6	0.1176	0.2951	3.4718	180.1466	1.0766
C7	0.1096	0.0969	3.6805	54.9056	0.9885
C8	0.1065	0.2364	4.6486	177.3282	0.4392
C9	0.1165	0.2039	3.3955	167.4695	0.4560
C10	0.3295	0.2557	1.8217	97.3328	0.7481
C11	0.1246	0.1869	3.0025	166.1757	1.0952
C12	0.1463	0.1883	2.8192	125.7393	0.7041
C13	0.1265	0.0867	3.9305	266.3277	0.4557
C14	0.1837	0.1212	5.8035	297.8893	0.3296
C15	0.1602	0.2467	5.5474	–272.6507	0.2211
C16	0.1722	0.1464	4.0653	107.0118	0.7248
Pentacene	0.0920	0.1270	0.0000	0.0000	1.4100
Coronene	0.1270	0.1550	0.0000	0.0000	0.8200
Urea	–	–	–	39.6975	

According to the results presented in Table 2 it can be seen that reorganization energies are in the range of ~0.1 eV to 0.4 eV. It can also be observed that the two most frequently investigated buckybowls, sumanene (structure 5) and corannulene (structure 1), have ~~significantly~~ higher reorganization energies than most of other buckybowls. At the same time, the lowest reorganization energy of holes has been calculated for buckybowl denoted with number 2, while the lowest reorganization energy of electrons has been found for the buckybowl denoted with number 13.

Hydrogen adsorption properties of buckybowls are becoming very popular. One of the first such studies was done by Scanlon et al. [52, 53], where hydrogen adsorption properties of corannulene (in this work denoted with number 1) via physisorption have been investigated in details employing both MP2 and molecular dynamics levels of theory. Their study was important because it emphasized that the specific charge distribution of corannulene and buckybowls in general, might be responsible for very competitive results when it comes to the adsorption based on physisorption. Later, competitive adsorption properties of the sumanene buckybowl (both modified and unmodified) towards various gas molecules have been demonstrated by other studies as well [12, 47, 54-56], including the detailed confirmation of physisorption mechanisms. Namely, it was confirmed that relatively high dipole moment of sumanene and corannulene buckybowls induce charge polarization in otherwise nonpolar molecules such as hydrogen, which enables its binding based on the electrostatic interactions. Such adsorption mechanism is of great importance because desorption could be achieved at lower temperature, thus allowing continuous use of buckybowls as binding agents [47, 52, 53].

Concerning the dipole moment, the results presented in Table 1 indicate that many more buckybowl structures have much higher dipole moments than corannulene and sumanene. This is clearly a significant stimulus for further studies of buckybowl's adsorption properties towards hydrogen. Namely, it can be seen in Table 2 that almost all investigated buckybowls have significantly higher dipole moments than corannulene and sumanene. In this regard buckybowls denoted with numbers 14 and 15 could be of particular significance, as their dipole moment is higher than 5 D, while their surfaces are much higher than corannulene's and sumanene's which certainly improves their adsorption capacities.

Hyperpolarizability is frequently used for the estimation of potential of some molecular structure in the area of non-linear optics (NLO) [57-60]. Namely, this quantity is frequently compared to that of the standard NLO medium, the urea molecule. If the value of

hyperpolarizability of certain molecule is higher than hyperpolarizability of urea molecule, it can be concluded that the investigated structure has certain potential for the application as nonlinear optical medium. According to the results presented in Table 2 it can be seen that hyperpolarizabilities of all buckybowls are significantly higher than hyperpolarizability of the urea molecule. The highest value of hyperpolarizability has been calculated for the buckybowl 14, in which case the hyperpolarizability was higher almost eight times. Of course, due to the specific geometries of pentacene and coronene, hyperpolarizability is absent in their cases, determining buckybowls as structures with much more potential to be applied in the area of NLO materials.

Beside reorganization energies, another important optoelectronic property is ΔE(S1–T1) gap. This quantity significantly determines the potential for exhibiting a so-called thermally activated delayed fluorescence (TADF) mechanism. This mechanism is important as it allows production of high efficiency OLED materials that are not based on the iridium or platinum complexes [61-63]. Although the usage of precious metal complexes makes possible to use usually non-radiative triplet excitons [64, 65], it is associated with a challenge related to the overall cost of such a methodology. This is the main reason why the TADF mechanism has significant advantage from the practical application standpoint. It is also important to emphasize that ΔE(S1–T1) values should be lower than ca. 0.37 eV, because in this case thermal population of S1 state is effective [66, 67]. ΔE(S1–T1) values of all buckybowls investigated in this work have been presented in Figure 5.

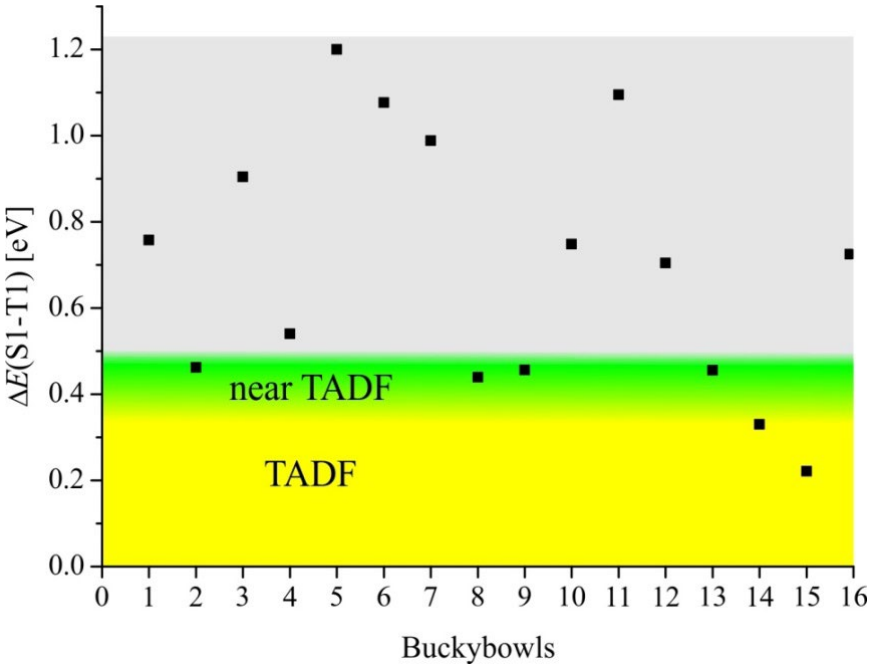

Figure 5. ΔE(S1–T1) values of all investigated buckybowls

The results shown in Figure 5 indicate that two buckybowls (14 and 15), allocated in the yellow region, have values below 0.37 eV and therefore possibly significant potential for application in TADF mechanism. Nevertheless, there are four more buckybowls (2, 8, 9, 13), indicated in green region, with ΔE(S1–T1) values very close to 0.37 eV. It is quite possible that ΔE(S1–T1) values of these buckybowls could be lowered to the desired 0.37 eV with structural adjustments. In comparison to flat carbon systems such as coronene, pentacene and other higher acenes it can be observed that buckybowls possess much higher potential for the application in the area of TADF. Namely, according to our previous results, the ΔE(S1–T1) value of pentacene is 1.41 eV [68]. This value decreases subsequently with the addition of benzene rings, but only to the value of 1.11 eV in the case of decacene, which is far away from 0.37 eV. Coronene, on the other hand, has much lower ΔE(S1–T1) value than pentacene and higher acenes, 0.82 eV, but that is also far away from 0.37 eV.

3.3. Charge transfer rates

Once the dimer structures have been obtained, the charge transfer integrals can be calculated which finally enables calculation of the charge transfer rates according to the equation (1). These results are presented in Table 3, for dimer structures obtained at both DFTB3-D3(BJ) and DFT/PBE-D3/DZP levels of theory.

As in the case of bowl depths and distances between buckybowls, we will again test the reliability of DFTB3-D3(BJ) for obtaining dimers by comparing the results with DFT-D3 level of theory. This is visualized in Figure 6.

Again, very good correlation between the results obtained with dimmers at DFTB3-D3(BJ) and DFT-D3 levels of theory can be observed. The only discrepancy can be seen in case of the dimer structure denoted with number 9. More specifically, the charge transfer rates in this case are different by one order of magnitude. This is a consequence of different mutual orientations of monomers, which is illustrated in Figure 2. Namely, it can be observed that monomers of 9 are mutually rotated and displaced in the case of structure obtained at the DFT-D3 level of theory, which explains the difference in the calculated values. As already mentioned in the Computational Details, there were some difficulties in optimization of this structure, thus eventually somewhat smaller basis set was used.

Table 3. Charge transfer rates of buckybowls investigated in this work

Dimers obtained @	DFTB3-D3(BJ)		DFT/PBE-D3	
	k_{CT}^{+} [s^{-1}]	k_{CT}^{-} [s^{-1}]	k_{CT}^{+} [s^{-1}]	k_{CT}^{-} [s^{-1}]
1	5.73×10^{08}	2.16×10^{08}	1.17×10^{7}	5.41×10^{07}
2	5.37×10^{10}	5.77×10^{10}	2.72×10^{11}	1.31×10^{10}
3	2.47×10^{14}	7.45×10^{13}	2.90×10^{14}	7.66×10^{13}
4	5.49×10^{13}	5.18×10^{13}	6.31×10^{13}	5.23×10^{13}
5	1.05×10^{08}	4.45×10^{10}	4.19×10^{08}	7.06×10^{10}
6	7.39×10^{10}	1.33×10^{13}	1.42×10^{10}	1.34×10^{13}
7	2.62×10^{10}	1.22×10^{15}	8.08×10^{09}	1.26×10^{15}
8	6.72×10^{13}	5.66×10^{11}	8.90×10^{13}	1.29×10^{12}
9	5.23×10^{14}	4.10×10^{12}	3.33×10^{13}	2.44×10^{13}
10	9.74×10^{12}	6.22×10^{13}	6.96×10^{12}	4.06×10^{13}
11	1.01×10^{14}	1.41×10^{13}	1.55×10^{14}	9.28×10^{12}
12	3.54×10^{14}	3.83×10^{13}	2.44×10^{14}	2.53×10^{13}
13	1.24×10^{14}	6.83×10^{14}	1.14×10^{14}	5.01×10^{14}
14	2.22×10^{14}	1.44×10^{15}	1.96×10^{14}	1.35×10^{15}
15	5.94×10^{13}	1.73×10^{14}	4.68×10^{13}	1.47×10^{14}
16	2.11×10^{14}	1.72×10^{14}	2.32×10^{14}	1.95×10^{14}
Pentacene	2.65×10^{14}	4.69×10^{11}	4.76×10^{13}	1.43×10^{14}
Coronene	1.95×10^{14}	6.17×10^{13}	1.00×10^{14}	5.66×10^{12}

Concerning the comparison between the curved and flat carbon systems, it can be seen that buckybowls exhibit very competitive charge transfer rates. Concerning the flat carbon systems, pentacene has significantly better charge transfer rates. For this study it, was very interesting to find out that there are buckybowls with k_{CT}^{+} and k_{CT}^{-} higher than for pentacene and coronene. More specifically, k_{CT}^{+} is higher in the case of buckybowl 12 than for the case of pentacene; for k_{CT}^{-}, buckybowls 16, 14, 13 and 7 have higher values than pentacene.

Pentacene and coronene have significantly lower values of reorganization energies and initially it could be concluded that this will lead to the charge transfer rates in favor of flat carbon systems. However, certain number of buckybowls has significantly better charge transfer rates. According to (1) used to calculate the charge transfer rates, it can be concluded that charge transfer integral, which depends on the orbital overlap, is much higher in the case of some buckybowls, therefore leading to the better charge transfer rates.

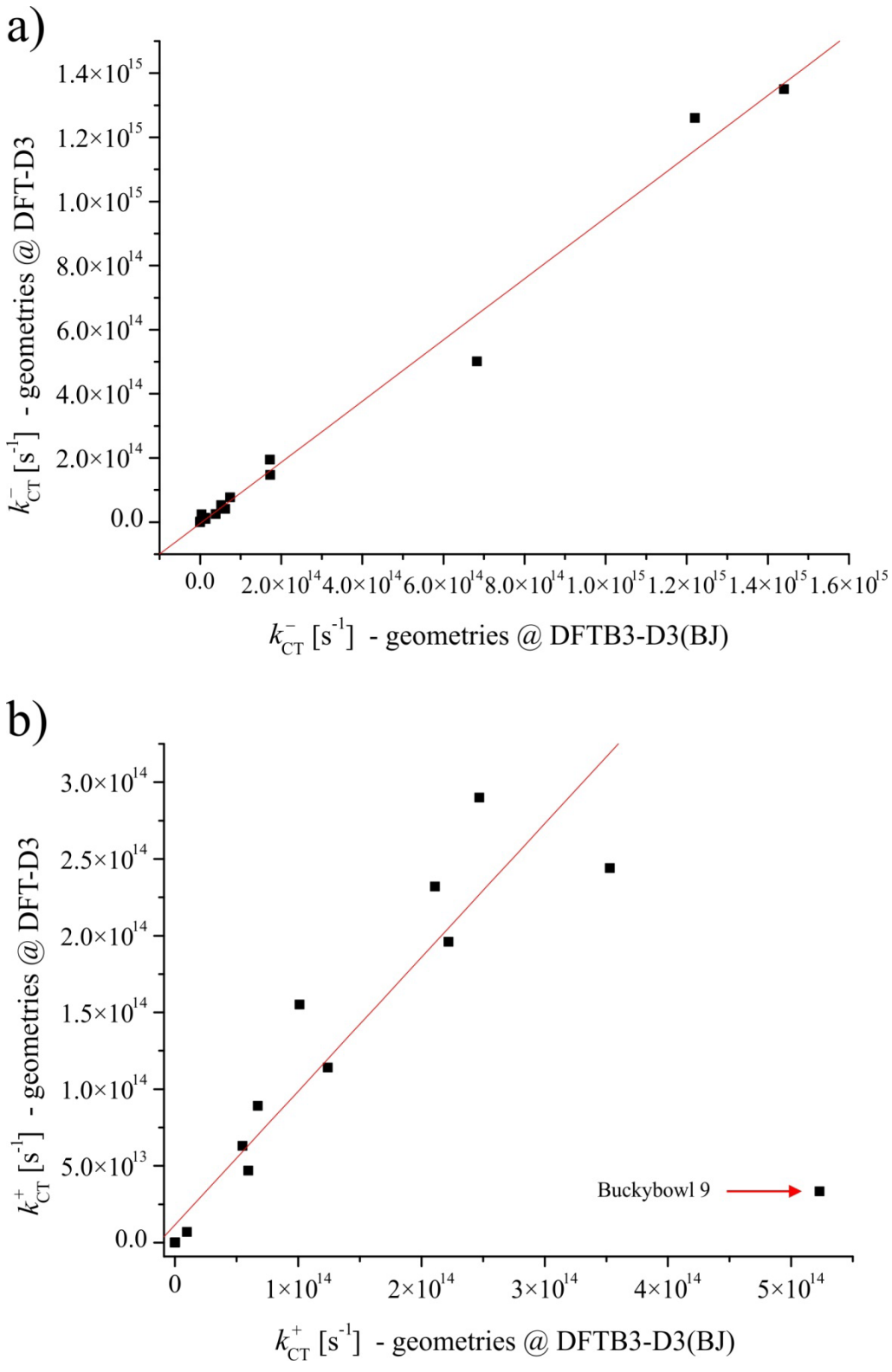

Figure 6. Charge transfer rates of a) electrons and b) holes, calculated for dimers obtained at two different levels of theory

3.4. Correlation of transfer rates with specific structural features of buckybowls

It was already shown that bowl depth as specific structural feature of buckybowls principally determines the b2b-i mechanism, which could be of great importance for the area of organic electronics. This is also very important because it substantially decreases the amount of time necessary to calculate the b2b-i barriers, which could be very tedious since it is necessary to locate the transition state. In this work we were also interested if bowl depth could also be correlated with charge transfer rates. Initial simple correlation of bowl depth to the fourth power with electron charge hopping, Figure 7, indicates substantial deviation of three bowls.

More detailed investigation reveals that these bowls are the ones with the highest charge hopping rates for electrons, thus indicating that more parameters should be included. At the same time, from the computational speed and efficiency standpoint, it would important to find a quantity that can be relatively easily obtained. One such quantity could be the number of noncovalent interactions between buckybowls in dimer structures, which in the Jaguar program is based on the method of Johnson et al. [69, 70]. The idea concerning the noncovalent interactions was as following. Charge transfer rates principally depend on the reorganization energies and charge coupling between buckybowls. The higher the orbital overlap between buckybowls, the higher will be the charge coupling. At the same time, the higher the electron density between buckybowls, the higher possibility for the transfer from one buckybowl to another. Finally, higher electron density between buckybowls will lead to the higher number of noncovalent interactions. Correlation between electron hopping rates and the ratio between number of noncovalent interactions (NCI) and bowl depth to the fourth power is presented in Figure 8.

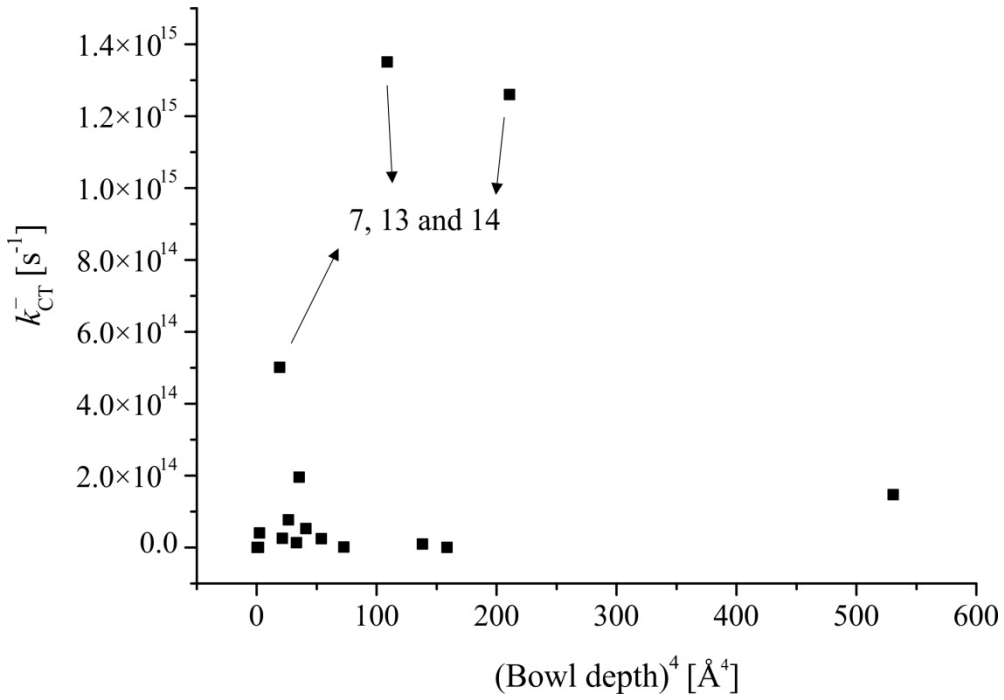

Figure 7. Correlation between electron hopping rates and bowl depth to the fourth power

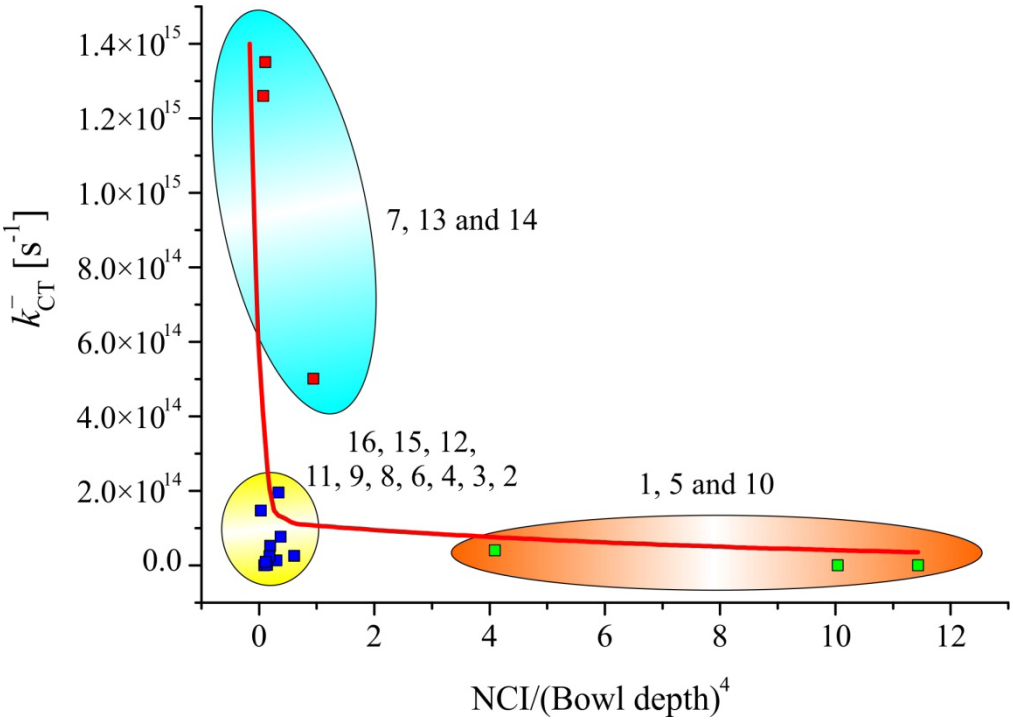

Figure 8. Correlation between electron hopping rates and ratio of number of NCI and bowl depth to the fourth power

Number and strength of NCI between two same molecules depend, in general, on their mutual orientation. On the other side mutual orientation of buckybowls depend on their main structural property – bowl depth, which leads to the conclusion that numbers of NCI and bowl depths are related. For this reason we decided to try with correlation between k_{CT}^{-} and ratio of NCI and bowl depths. Additionally, Bürgi and Dubler-Steudle [71] and Priyakumar and Sastry [42] have demonstrated the importance of the bowl depth to the fourth power. Namely, they have shown by calculations related to double well potential that bowl depth to the fourth power nicely correlates with b2b-i. Therefore, we decided to try correlations with bowl depth to the fourth power.

Inspection of Figure 8 indicates that there exists an excellent correlation between electron hopping rates and ratio of NCI and bowl depths to the fourth power, in the form of the second-order exponential decay. Three regions can be identified. In the blue area, buckybowls 7, 13 and 14 are located and these buckybowls are characterized by the lowest electron reorganization energies and electron transfer rates significantly better than the ones obtained for pentacene and coronene. In the yellow region, the highest number of buckybowls is located with an average electron reorganization energy of 0.22 eV and electron transfer rates that are very competitive to the values obtained for pentacene and coronene. Finally, the brown region contains three buckybowls, sumanene, corannulene and buckybowl 10, with the lowest values of bowl depths.

4. Conclusion

A fast and efficient DFTB3-D3(BJ) method has been validated for the optimization of representative buckybowls and for the obtaining of their dimer structures. The results have been compared with the DFT/PBE-D3 level of theory. Further, optoelectronic properties buckybowls have been assessed by calculation of reorganization energies, ΔE(S1–T1) values, first hyperpolarizabilities and charge hopping rates. Reorganization energies of buckybowls are significantly higher than in the case of pentacene and coronene. On the other hand, the ΔE(S1–T1) values for two buckybowls are lower than 0.37 eV and, at the same time, much lower than the corresponding values for pentacene and coronene. Hyperpolarizabilities of buckybowls are much higher comparing with urea molecule, indicating potential for application in the field of NLO. Finally, it has been shown that certain buckybowls have charge transfer rates significantly

better than in the case of pentacene and coronene, further emphasizing the potential of buckybowls. Furthermore, an effort has been made in order to correlate specific structural properties of buckybowls with electron transfer rates. Namely, it has been shown that very good correlation in the form of the second-order exponential decay exists between the electron transfer rates and the ratio of the number of NCI and bowl depth to the fourth power. Once again, bowl depth turned out to have a significant influence on important properties, in this case electron hopping rates. Methodology applied in this work and the obtained correlation allows relatively fast assessment of electron transfer rates in case of buckybowls.

Acknowledgment

This work has been performed thanks to the support received from Schrödinger Inc. This study was conducted within the projects supported by the Ministry of Education, Science and Technological Development of Serbia, grant numbers OI 171039 and TR 34019 (project period 2016-2019/20).

References

1. Purushotham, U. and Sastry, G.N., 2013. Conjugate acene fused buckybowls: evaluating their suitability for p-type, ambipolar and n-type air stable organic semiconductors. Physical Chemistry Chemical Physics. **15**(14), 5039-5048.
2. Sakurai, H., Daiko, T., and Hirao, T., 2003. A synthesis of sumanene, a fullerene fragment. Science. **301**(5641), 1878-1878.
3. Sakurai, H., Daiko, T., Sakane, H., Amaya, T., and Hirao, T., 2005. Structural elucidation of sumanene and generation of its benzylic anions. Journal of the American Chemical Society. **127**(33), 11580-11581.
4. Mebs, S., Weber, M., Luger, P., Schmidt, B.M., Sakurai, H., Higashibayashi, S, et al., 2012. Experimental electron density of sumanene, a bowl-shaped fullerene fragment; comparison with the related corannulene hydrocarbon. Organic & biomolecular chemistry. **10**(11), 2218-2222.
5. Barth, W.E. and Lawton, R.G., 1966. Dibenzo [ghi, mno] fluoranthene. Journal of the American Chemical Society. **88**(2), 380-381.
6. Lawton, R.G. and Barth, W.E., 1971. Synthesis of corannulene. Journal of the American Chemical Society. **93**(7), 1730-1745.
7. Priyakumar, U.D. and Sastry, G.N., 2001. Theory provides a clue to accomplish the synthesis of sumanene, C 21 H 12, the prototypical C 3v-buckybowl. Tetrahedron Letters. **42**(7), 1379-1381.
8. Higashibayashi, S. and Sakurai, H., 2011. Synthesis of sumanene and related buckybowls. Chemistry Letters. **40**(2), 122-128.
9. Amaya, T., Sakane, H., and Hirao, T., 2007. A Concave-Bound CpFe Complex of Sumanene as a Metal in a π Bowl. Angewandte Chemie. **119**(44), 8528-8531.

10. Amaya, T., Nakata, T., and Hirao, T., 2009. Synthesis of Highly Strained π-Bowls from Sumanene. Journal of the American Chemical Society. **131**(31), 10810-10811.
11. Wu, T.-C., Hsin, H.-J., Kuo, M.-Y., Li, C.-H., and Wu, Y.-T., 2011. Synthesis and structural analysis of a highly curved Buckybowl containing corannulene and sumanene fragments. Journal of the American Chemical Society. **133**(41), 16319-16321.
12. Armaković, S., Armaković, S.J., and Šetrajčić, J.P., 2013. Hydrogen storage properties of sumanene. international journal of hydrogen energy. **38**(27), 12190-12198.
13. Spisak, S.N., Zabula, A.V., Filatov, A.S., Rogachev, A.Y., and Petrukhina, M.A., 2011. Selective Endo and Exo Binding of Alkali Metals to Corannulene. Angewandte Chemie International Edition. **50**(35), 8090-8094.
14. Filatov, A.S., Ferguson, M.V., Spisak, S.N., Li, B., Campana, C.F., and Petrukhina, M.A., 2013. Bowl-shaped polyarenes as concave–convex shape complementary hosts for C60-and C70-fullerenes. Crystal Growth & Design. **14**(2), 756-762.
15. Amaya, T. and Hirao, T., 2011. A molecular bowl sumanene. Chemical Communications. **47**(38), 10524-10535.
16. Amaya, T., Sakane, H., Muneishi, T., and Hirao, T., 2008. Bowl-to-bowl inversion of sumanene derivatives. Chemical Communications, (6), 765-767.
17. Amaya, T., Sakane, H., Nakata, T., and Hirao, T., 2010. A theoretical study of the bowl-to-bowl inversion of sumanene derivatives. Pure and Applied Chemistry. **82**(4), 969-978.
18. Armaković, S., Armaković, S.J., Šetrajčić, J.P., and Šetrajčić, I.J., 2013. Optical and bowl-to-bowl inversion properties of sumanene substituted on its benzylic positions; a DFT/TD-DFT study. Chemical Physics Letters. **578**, 156-161.
19. Imamura, K., Takimiya, K., Otsubo, T., and Aso, Y., 1999. Triphenyleno [1, 12-bcd: 4, 5-b′ c′ d′: 8, 9-b ″c ″d ″] trithiophene: the first bowl-shaped heteroaromatic. Chemical Communications, (18), 1859-1860.
20. Amaya, T., Seki, S., Moriuchi, T., Nakamoto, K., Nakata, T., Sakane, H., et al., 2008. Anisotropic electron transport properties in sumanene crystal. Journal of the American Chemical Society. **131**(2), 408-409.
21. Higashibayashi, S., Tsuruoka, R., Soujanya, Y., Purushotham, U., Sastry, G.N., Seki, S., et al., 2012. Trimethylsumanene: enantioselective synthesis, substituent effect on bowl structure, inversion energy, and electron conductivity. Bulletin of the chemical society of Japan. **85**(4), 450-467.
22. Miyajima, D., Tashiro, K., Araoka, F., Takezoe, H., Kim, J., Kato, K., et al., 2008. Liquid crystalline corannulene responsive to electric field. Journal of the American Chemical Society. **131**(1), 44-45.
23. Akasaka, T., Osuka, A., Fukuzumi, S., Kandori, H., and Aso, Y., *Chemical Science of [pi]-Electron Systems*. 2015: Springer.
24. Josa, D., González-Veloso, I., Rodríguez-Otero, J., and Cabaleiro-Lago, E.M., 2015. Tailoring buckybowls for fullerene recognition. A dispersion-corrected DFT study. Physical Chemistry Chemical Physics. **17**(9), 6233-6241.
25. *Schrödinger Materials Science User Manual*. 2014, Schrödinger Press.
26. te Velde, G., Bickelhaupt, F.M., Baerends, E.J., Fonseca Guerra, C., van Gisbergen, S.J.A., Snijders, J.G., and Ziegler, T., 2001. Chemistry with ADF. Journal of Computational Chemistry. **22**(9), 931-967.
27. Fonseca Guerra, C., Snijders, G.J., te Velde, G., and Baerends, J.E., 1998. Towards an order-N DFT method. Theoretical Chemistry Accounts. **99**(6), 391-403.

28. E.J. Baerends, T. Ziegler, A.J. Atkins, J. Autschbach, D. Bashford, A. Bérces, et al., *ADF2016, SCM, Theoretical Chemistry, Vrije Universiteit, Amsterdam, The Netherlands, http://www.scm.com.* . 2016.
29. Becke, A.D., 1993. Density-functional thermochemistry. III. The role of exact exchange. The Journal of chemical physics. **98**(7), 5648-5652.
30. Armaković, S., Armaković, S.J., Pelemiš, S.S., and Šetrajčić, J.P., 2015. Optoelectronic and charge carrier hopping properties of ultra-thin boron nitride nanotubes. Superlattices and Microstructures. **79**, 79-85.
31. A. Yakovlev, P. Philipsen, S. Borini, R. Rüger, A. F. Oliveira, M. de Reus, et al., *ADF DFTB 2016, SCM, Theoretical Chemistry, Vrije Universiteit, Amsterdam, The Netherlands, http://www.scm.com*. 2016.
32. Elstner, M., Porezag, D., Jungnickel, G., Elsner, J., Haugk, M., Frauenheim, T., et al., 1998. Self-consistent-charge density-functional tight-binding method for simulations of complex materials properties. Physical Review B. **58**(11), 7260-7268.
33. Niehaus, T.A., Elstner, M., Frauenheim, T., and Suhai, S., 2001. Application of an approximate density-functional method to sulfur containing compounds. Journal of Molecular Structure: THEOCHEM. **541**(1–3), 185-194.
34. Gaus, M., Cui, Q., and Elstner, M., 2011. DFTB3: Extension of the Self-Consistent-Charge Density-Functional Tight-Binding Method (SCC-DFTB). Journal of Chemical Theory and Computation. **7**(4), 931-948.
35. Gaus, M., Goez, A., and Elstner, M., 2013. Parametrization and Benchmark of DFTB3 for Organic Molecules. Journal of Chemical Theory and Computation. **9**(1), 338-354.
36. Van Lenthe, E. and Baerends, E.J., 2003. Optimized Slater-type basis sets for the elements 1–118. Journal of Computational Chemistry. **24**(9), 1142-1156.
37. Autschbach, J., 2009. Magnitude of Finite-Nucleus-Size Effects in Relativistic Density Functional Computations of Indirect NMR Nuclear Spin–Spin Coupling Constants. ChemPhysChem. **10**(13), 2274-2283.
38. Bérces, A., Dickson, R.M., Fan, L., Jacobsen, H., Swerhone, D., and Ziegler, T., 1997. An implementation of the coupled perturbed Kohn-Sham equations: perturbation due to nuclear displacements. Computer Physics Communications. **100**(3), 247-262.
39. Jacobsen, H., Bérces, A., Swerhone, D.P., and Ziegler, T., 1997. Analytic second derivatives of molecular energies: a density functional implementation. Computer Physics Communications. **100**(3), 263-276.
40. Wolff, S.K., 2005. Analytical second derivatives in the Amsterdam density functional package. International Journal of Quantum Chemistry. **104**(5), 645-659.
41. Priyakumar, U.D. and Sastry, G.N., 2001. First ab initio and density functional study on the structure, bowl-to-bowl inversion barrier, and vibrational spectra of the elusive C 3 v-Symmetric Buckybowl: Sumanene, C21H12. The Journal of Physical Chemistry A. **105**(18), 4488-4494.
42. Priyakumar, U.D. and Sastry, G.N., 2001. Heterobuckybowls: a theoretical study on the structure, bowl-to-bowl inversion barrier, bond length alternation, structure-inversion barrier relationship, stability, and synthetic feasibility. The Journal of organic chemistry. **66**(20), 6523-6530.
43. Sastry, G.N., Rao, H.S.P., Bednarek, P., and Priyakumar, U.D., 2000. Effect of substitution on the curvature and bowl-to-bowl inversion barrier of bucky-bowls. Study of mono-substituted corannulenes (C19XH10, X= B−, N+, P+ and Si). Chemical Communications,

(10), 843-844.
44. Armaković, S., Armaković, S.J., Šetrajčić, J.P., and Džambas, L.D., 2013. Specificities of boron disubstituted sumanenes. Journal of molecular modeling. **19**(3), 1153-1166.
45. Grimme, S., Antony, J., Ehrlich, S., and Krieg, H., 2010. A consistent and accurate ab initio parametrization of density functional dispersion correction (DFT-D) for the 94 elements H-Pu. The Journal of chemical physics. **132**(15), 154104.
46. Grimme, S., Ehrlich, S., and Goerigk, L., 2011. Effect of the damping function in dispersion corrected density functional theory. Journal of computational chemistry. **32**(7), 1456-1465.
47. Armaković, S., Armaković, S.J., Pelemiš, S., and Mirjanić, D., 2016. Influence of sumanene modifications with boron and nitrogen atoms to its hydrogen adsorption properties. Physical Chemistry Chemical Physics. **18**(4), 2859-2870.
48. García, G., Moral, M., Garzón, A., Granadino-Roldán, J.M., Navarro, A., and Fernández-Gómez, M., 2012. Poly (arylenethynyl-thienoacenes) as candidates for organic semiconducting materials. A DFT insight. Organic Electronics. **13**(12), 3244-3253.
49. Evans, D.R., Kwak, H.S., Giesen, D.J., Goldberg, A., Halls, M.D., and Oh-e, M., 2016. Estimation of charge carrier mobility in amorphous organic materials using percolation corrected random-walk model. Organic Electronics. **29**, 50-56.
50. Wang, L., Nan, G., Yang, X., Peng, Q., Li, Q., and Shuai, Z., 2010. Computational methods for design of organic materials with high charge mobility. Chemical Society Reviews. **39**(2), 423-434.
51. Coropceanu, V., Cornil, J., da Silva Filho, D.A., Olivier, Y., Silbey, R., and Brédas, J.-L., 2007. Charge transport in organic semiconductors. Chemical Reviews. **107**(4), 926-952.
52. Scanlon, L., Feld, W., Balbuena, P., Sandi, G., Duan, X., Underwood, K. et al., 2009. Hydrogen storage based on physisorption. The Journal of Physical Chemistry B. **113**(14), 4708-4717.
53. Scanlon, L., Balbuena, P., Zhang, Y., Sandi, G., Back, C., Feld, W. et al., 2006. Investigation of corannulene for molecular hydrogen storage via computational chemistry and experimentation. The Journal of Physical Chemistry B. **110**(15), 7688-7694.
54. Armaković, S., Armaković, S.J., Šetrajčić, J.P., Jaćimovski, S.K., and Holodkov, V., 2014. Sumanene and its adsorption properties towards CO, CO2 and NH3 molecules. Journal of molecular modeling. **20**(4), 1-14.
55. Reisi-Vanani, A., Hamadanian, M., and Kokhdan, S.N., 2016. Functionalization of the sumanene by nitrous oxide: A mechanistic study. Computational and Theoretical Chemistry. **1082**, 49-57.
56. Reisi-Vanani, A. and Mehrdoust, S., 2016. Effect of boron doping in sumanene frame toward hydrogen physisorption: A theoretical study. International Journal of Hydrogen Energy.
57. Joseph, T., Varghese, H.T., Panicker, C.Y., Thiemann, T., Viswanathan, K., Van Alsenoy, C., and Manojkumar, T., 2014. Spectroscopic (FT-IR, FT-Raman), first order hyperpolarizability, NBO analysis, HOMO and LUMO analysis of 2, 4-bis (2-methoxyphenyl)-1-phenylanthracene-9, 10-dione by ab initio HF and density functional methods. Spectrochimica Acta Part A: Molecular and Biomolecular Spectroscopy. **117**, 413-421.
58. Raju, R., Panicker, C.Y., Nayak, P.S., Narayana, B., Sarojini, B., Van Alsenoy, C., and Al-Saadi, A.A., 2015. FT-IR, molecular structure, first order hyperpolarizability, MEP, HOMO and LUMO analysis and NBO analysis of 4-[(3-acetylphenyl) amino]-2-methylidene-4-oxobutanoic acid. Spectrochimica Acta Part A: Molecular and Biomolecular Spectroscopy.

134, 63-72.
59. Kumar, C.C., Panicker, C.Y., Fun, H.-K., Mary, Y.S., Harikumar, B., Chandraju, S., et al. 2014. FT-IR, molecular structure, first order hyperpolarizability, HOMO and LUMO analysis, MEP and NBO analysis of 2-(4-chlorophenyl)-2-oxoethyl 3-nitrobenzoate. Spectrochimica Acta Part A: Molecular and Biomolecular Spectroscopy. **126**, 208-219.
60. Mary, Y.S., Raju, K., Panicker, C.Y., Al-Saadi, A.A., and Thiemann, T., 2014. Molecular conformational analysis, vibrational spectra, NBO analysis and first hyperpolarizability of (2E)-3-(3-chlorophenyl) prop-2-enoic anhydride based on density functional theory calculations. Spectrochimica Acta Part A: Molecular and Biomolecular Spectroscopy. **131**, 471-483.
61. Jankus, V., Data, P., Graves, D., McGuinness, C., Santos, J., Bryce, M.R., Dias, F.B., et al. 2014. Highly efficient TADF OLEDs: How the emitter–host interaction controls both the excited state species and electrical properties of the devices to achieve near 100% triplet harvesting and high efficiency. Advanced Functional Materials. **24**(39), 6178-6186.
62. Wu, S., Aonuma, M., Zhang, Q., Huang, S., Nakagawa, T., Kuwabara, K. et al. 2014. High-efficiency deep-blue organic light-emitting diodes based on a thermally activated delayed fluorescence emitter. Journal of Materials Chemistry C. **2**(3), 421-424.
63. Dias, F.B., Bourdakos, K.N., Jankus, V., Moss, K.C., Kamtekar, K.T., Bhalla, V. et al. 2013. Triplet harvesting with 100% efficiency by way of thermally activated delayed fluorescence in charge transfer OLED emitters. Advanced Materials. **25**(27), 3707-3714.
64. Baldo, M., Lamansky, S., Burrows, P., Thompson, M., and Forrest, S., 1999. Very high-efficiency green organic light-emitting devices based on electrophosphorescence. Applied Physics Letters. **75**, 4.
65. Uoyama, H., Goushi, K., Shizu, K., Nomura, H., and Adachi, C., 2012. Highly efficient organic light-emitting diodes from delayed fluorescence. Nature. **492**(7428), 234-238.
66. Linfoot, C.L., Leitl, M.J., Richardson, P., Rausch, A.F., Chepelin, O., White, F.J. et al., 2014. Thermally Activated Delayed Fluorescence (TADF) and Enhancing Photoluminescence Quantum Yields of [CuI (diimine)(diphosphine)]+ Complexes□ Photophysical, Structural, and Computational Studies. Inorganic chemistry. **53**(20), 10854-10861.
67. Leitl, M.J., Krylova, V.A., Djurovich, P.I., Thompson, M.E., and Yersin, H., 2014. Phosphorescence versus Thermally Activated Delayed Fluorescence. Controlling Singlet–Triplet Splitting in Brightly Emitting and Sublimable Cu (I) Compounds. Journal of the American Chemical Society. **136**(45), 16032-16038.
68. Armaković, S., Armaković, S.J., Holodkov, V., and Pelemiš, S., 2016. Optoelectronic properties of higher acenes, their BN analogue and substituted derivatives. Materials Chemistry and Physics. **170**, 210-217.
69. Otero-de-la-Roza, A., Johnson, E.R., and Contreras-García, J., 2012. Revealing non-covalent interactions in solids: NCI plots revisited. Physical Chemistry Chemical Physics. **14**(35), 12165-12172.
70. Johnson, E.R., Keinan, S., Mori-Sanchez, P., Contreras-Garcia, J., Cohen, A.J., and Yang, W., 2010. Revealing noncovalent interactions. Journal of the American Chemical Society. **132**(18), 6498-6506.
71. Bürgi H-B, Dubler-Steudle K.C., 1988. Empirical potential energy surfaces relating structure and activation energy. 1. Metallacyclopentene ring inversion in (s-cis-η4-butadiene)metallocene complexes and related compounds. Journal of the American Chemical Society **110,** 4953–4957.